

Article

Preparation and Magneto-Structural Investigation of Nanocrystalline CoMn-Based Heusler Alloy Glass-Coated Microwires

Mohamed Salaheldeen ^{1,2,3,4,*} , Ahmed Talaat ^{1,2,4} , Mihail Ipatov ^{1,2,4} , Valentina Zhukova ^{1,2,4} 
and Arcady Zhukov ^{1,2,4,5,*} 

- ¹ Departamento de Polímeros y Materiales Avanzados, Facultad Química, Universidad del País Vasco, UPV/EHU, 20018 San Sebastian, Spain
² Departamento de Física Aplicada, EIG, Universidad del País Vasco, UPV/EHU, 20018 San Sebastian, Spain
³ Physics Department, Faculty of Science, Sohag University, Sohag 82524, Egypt
⁴ EHU Quantum Center, University of the Basque Country, UPV/EHU, 48940 Leioa, Spain
⁵ IKERBASQUE, Basque Foundation for Science, 48011 Bilbao, Spain
* Correspondence: mohamed.salaheldeenmohamed@ehu.eus (M.S.); arkadi.joukov@ehu.eus (A.Z.)

Abstract: In this work, we have successfully fabricated nanocrystalline Co₂MnSi Heusler alloy glass-coated microwires with a metallic nucleus diameter (d_{nuclei}) $10.2 \pm 0.1 \mu\text{m}$ and total diameter $22.2 \pm 0.1 \mu\text{m}$ by the Taylor–Ulitsky technique for the first time. Magnetic and structural investigations have been performed to clarify the basic magneto-structural properties of the Co₂MnSi glass-coated microwires. XRD showed a well-defined crystalline structure with a lattice parameter $a = 5.62 \text{ \AA}$. The room temperature magnetic behavior showed a strong in-plane magnetocrystalline anisotropy parallel to the microwire axis. The M-H loops showed unique thermal stability with temperature where the coercivity (H_c) and normalized magnetic remanence exhibited roughly stable tendency with temperature. Moreover, quite soft magnetic behavior has been observed with values of coercivity of the order of $H_c = 7 \pm 2 \text{ Oe}$. Zero field cooling and field cooling (ZFC-FC) magnetization curves displayed notable irreversible magnetic dependence, where a blocking temperature ($T_B = 150 \text{ K}$) has been observed. The internal stresses generated during the fabrication process induced a different magnetic phase and is responsible for the irreversibility behavior. Moreover, high Curie temperature has been reported ($T_c \approx 985 \text{ K}$) with unique magnetic behavior at a wide range of temperature and magnetic fields, making it a promising candidate in magnetic sensing and spintronic applications.



Citation: Salaheldeen, M.; Talaat, A.; Ipatov, M.; Zhukova, V.; Zhukov, A. Preparation and Magneto-Structural Investigation of Nanocrystalline CoMn-Based Heusler Alloy Glass-Coated Microwires. *Processes* **2022**, *10*, 2248. <https://doi.org/10.3390/pr10112248>

Academic Editor: Prashant K. Sarswat

Received: 6 October 2022

Accepted: 28 October 2022

Published: 1 November 2022

Publisher's Note: MDPI stays neutral with regard to jurisdictional claims in published maps and institutional affiliations.



Copyright: © 2022 by the authors. Licensee MDPI, Basel, Switzerland. This article is an open access article distributed under the terms and conditions of the Creative Commons Attribution (CC BY) license (<https://creativecommons.org/licenses/by/4.0/>).

Keywords: Co₂MnSi Heusler alloys; magnetic properties; glass-coated microwires; blocking temperature; thermal stability; spintronic

1. Introduction

Ferromagnetic materials with high spin polarization ($\approx 100\%$) have attracted special and considerable attention due to their wide range of applications in the field of spintronics, magneto-optics and thermoelectricity [1]. Full and half Heusler alloys, because of their unique electronic structures which support up to 100% spin polarization, are of particular interest [2–4]. In this class of materials, the majority spin band has a metallic behavior, whereas the minority spin band has semiconducting or insulating properties because of the existence of a bandgap around the Fermi energy [5]. Thus, these materials perform 100% spin polarized at the Fermi energy.

Among Heusler alloys, Co-based Heusler compounds are very promising materials for multifunction applications due to low magnetic damping coefficients, high Curie point ($T_c > 1200 \text{ K}$), tunable band structure and high magnetic moment [6–8]. In addition, such alloys present extraordinary and anomalous physical properties above and below

room temperature due to the large Berry curvature linked with their band structure [9,10]. Therefore, Co-based Heusler compounds are widely studied and investigated by many researchers around the world.

Among Heusler alloys based on 3d transition elements (especially, Co), Co_2MnSi is of particular interest for advanced spintronic devices because of its large bandgap for minority spins (0.5 to 0.8 eV), high Curie temperature (~ 985 K), high tunnel magnetoresistance, large magnetoresistance ratios and perpendicular magnetic anisotropy [11–14]. Both the experimental and theoretical investigation conducted on Co_2MnSi over the last two decades have been focused on the structural and magnetic properties and their relation to spin polarization [11,15–17]. The highest spin polarization value that has been observed for bulk Co_2MnSi is $\sim 93\%$ at room temperature by ultraviolet photoemission spectroscopy [18]. The Co_2MnSi Heusler alloy is considered one of the most studied Co-based Heusler compounds and a promising material for spintronic application.

The most common technique for preparing and fabricating magnetic Heusler alloys is arc melting followed by thermal treatment [19,20]. This method allows one to prepare bulk Heusler alloys with tunable chemical compositions. Moreover, different techniques are supposed to obtain Heusler alloys with varied forms such as thin films, nanoparticles, ribbons and nanostructured materials as reported elsewhere [21].

Many physical properties of bulk Heusler alloys can be tailored and improved by miniaturization as described elsewhere [22–25]. However, preparation of all perspective “multifunctional and smart” Heusler alloys faces several problems and challenges. Firstly, large-scale production of Heusler compounds alloys with exact chemical composition and reproducible physical properties. In addition, the high cost of specific techniques that require extreme high physical constrains and conditions (ultra-high vacuum, pressure, power, high temperature and specific substrate). Therefore, the recent upgrade of the Taylor–Ulitovsky method, which allows preparation of ultra-thin and homogenous glass-coated microwires—a composite material consisting of a metallic nucleus (diameter ~ 0.1 – 100 μm) covered with a glass coating (thickness ~ 2 – 30 μm) has recently attracted considerable attention [26]. The low cost for large-scale production (i.e., several kilometers from a small ingot (~ 5 g)) makes it a very promising technique for fabrication of multifunctional and smart materials for a wide range of applications. In addition, the possibility of preparation glass-coated microwires with different structures (amorphous, nano-crystalline, and granular) provides a unique advantage to investigate the effect of different microstructures of the same material on its physical properties [27–33]. Moreover, the glass-coating layer offers insulation from electrical short-circuit, which allows the microwire to be used in a chemically aggressive environment. Thus, glass-coated microwires are strongly used in biomedical applications and hyperthermia for in vitro cancer cell treatment [34–36].

Despite numerous investigations of the different physical properties of Co_2MnSi alloys with different physical forms, not many studies that deal with Co_2MnSi -based glass coated microwires are reported. In the present study, we try to investigate the magneto-structural properties of Co_2MnSi glass-coated microwires prepared by the Taylor–Ulitovsky technique. The basic magnetic and structural characterization have been performed. The XRD analysis proves the existence of a nanocrystalline $L2_1$ ordered structure beside the disordered B2 and amorphous phases. The M-H loops show thermal stability at a wide range of temperature, where the value of coercivity and the remanence did not show noticeable differences. In addition, the investigation of the temperature dependence of the magnetization has indicated the presence of the magnetic phase transition at low temperature. Moreover, we show that it is possible to produce up to kilometres of nanocrystalline Co_2MnSi Heusler-based glass-coated microwires simply/rapidly/at low cost by using the Taylor–Ulitovsky method that may enhance the suitability of Co_2MnSi for sensing and microspintronic-based devices.

2. Materials and Methods

The fabrication of Co_2MnSi glass-coated microwires with a nominal ratio (2:1:1), i.e., $\text{Co}_{50}\text{Mn}_{25}\text{Si}_{25}$ was quite a challenge due to the easy evaporation of Mn which will effect the real nominal composition ratio. Therefore, we started preparing the Co_2MnSi alloy by using a commercial arc furnace with an Mn excess. We have performed the melting from highly pure elements, Co (99.99%), Si (99.9%) and Mn (99.99%) under vacuum and in an argon atmosphere to avoid the Co_2MnSi alloy from oxidation during the melting process. The melting process was repeated five times to have homogenous alloys of Co_2MnSi . Then we checked the nominal chemical composition of the Co_2MnSi alloys by using energy dispersive X-ray (EDX)/ scanning electron microscopy (SEM). After we confirmed the nominal ratio (2(Co):1(Mn):1(Si)) we started the fabrication of the Co_2MnSi glass-coated microwires by using the Taylor–Ulitsky technique, which consists on drawing and casting directly from the melted $\text{Co}_{50}\text{Mn}_{25}\text{Si}_{25}$ alloy as described in detail elsewhere [37,38]. Briefly, an ingot was heated above its melting temperature by a high frequency inductor, and then a glass capillary formed, which was filled with molten Co_2MnSi alloy, drawn out and wound onto a rotating pick-up bobbin [39]. The speed of the wire drowning and the velocity of the rotation of the pick-up bobbin controlled the diameter of the metallic nuclei, d . In addition, rapid melt quenching is achieved by a stream of coolant, when the formed microwire passes through a coolant stream [40]. By using scanning electron microscopy, SEM, (see Figure 1a,c) we estimate the geometric parameters of Co_2MnSi glass-coated microwires where the metallic nucleus diameter of the prepared Co_2MnSi microwire is $d_{\text{nuclei}} = 10.2 \pm 0.1 \mu\text{m}$ and the total diameter $D_{\text{total}} = 22.2 \pm 0.1 \mu\text{m}$. The most interesting part in fabrication process is that the metallic nuclei is surrounded by the glass coating during the rapid solidification process to prevent the metallic nuclei from the oxidation, so it is an ideal technique for Mn-based alloys. Moreover, such a process is associated with elevated internal stresses arising from the rapid quenching itself, drawing and from the different thermal expansion coefficients of the glass and the metallic nucleus and adding additional internal stress [41,42].

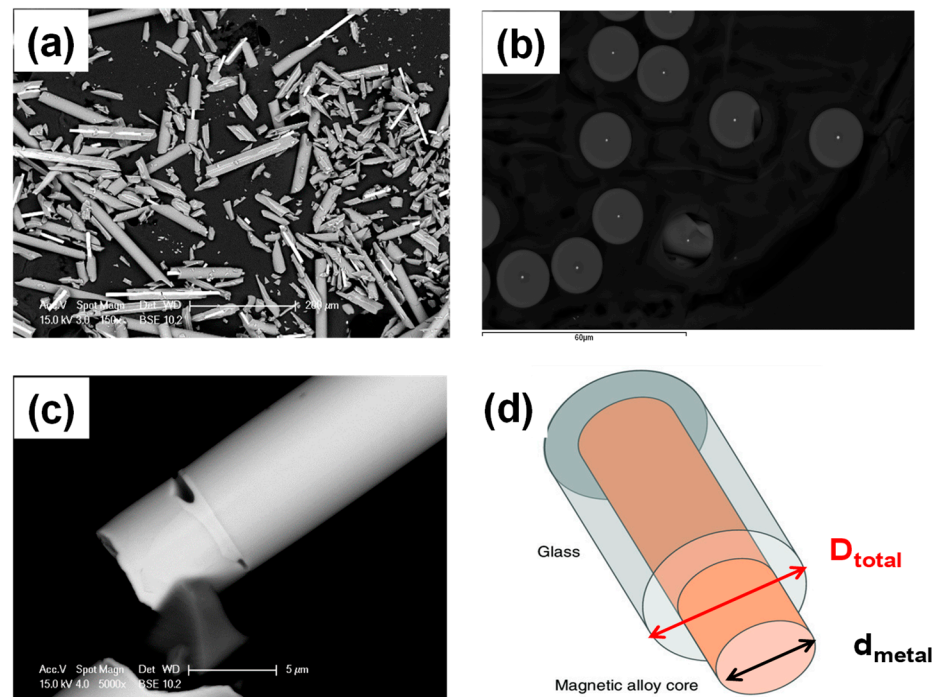


Figure 1. SEM image of Co_2MnSi glass-coated microwire (a) and its cross section (b). (c) High magnification of a single glass coated microwire and (d) indicates the formation of Co_2MnSi glass-coated microwires, sketch.

We checked the chemical composition of the as-prepared samples with energy dispersive X-ray spectroscopy (EDX). The real chemical composition is obtained from analysis of 10 different points as described in Figure 1b and the average of the chemical composition is about ($\text{Co}_{51}\text{Mn}_{23.9}\text{Si}_{25.1}$), i.e., the nominal ratio (2:1:1) is approved.

The investigation of the microstructure of Co_2MnSi glass-coated microwires and its phase analysis have been conducted by using X-ray diffraction (XRD) BRUKER (D8 Advance, Bruker AXS GmbH, Karlsruhe, Germany). The $\text{Cu K}\alpha$ ($\lambda = 1.54 \text{ \AA}$) radiation has been used in all the patterns.

Room temperature and thermal magnetic behavior of Co_2MnSi glass-coated microwire samples has been performed by using the physical property magnetic system, PPMS (Quantum Design Inc., San Diego, CA, USA) for the field cooling and zero-field cooling magnetization curves for a temperature range from 5–350 K with an applied external magnetic field of 100 Oe.

3. Results

3.1. Morphological and Structure Properties

Figure 1 describes the morphological properties of the as-prepared Co_2MnSi glass-coated microwires, which have been performed by SEM. As shown in Figure 1b, a perfect cylindrical shape is observed which reveals the homogenous distribution of Co_2MnSi .

Figure 2 shows the XRD analysis of the as-prepared Co_2MnSi glass-coated microwires. A wide halo centered on a $2\theta \approx 20^\circ$ peak related to the presence of an amorphous phase is combined with a narrow peak at the same angle related to the ordered $L2_1$ cubic phase with (220). The main source of the amorphous phase is the rapid melt quenching associated with the Taylor–Ulitsky fabrication method [27]. In addition, a very narrow peak at $2\theta \approx 45.6^\circ$ is detected that corresponds to the highly ordered $L2_1$ cubic structure (space group: $Fm\text{-}3m$). In addition, other peaks with (111) and (200) for $2\theta \approx 24^\circ$ and $2\theta \approx 27^\circ$, respectively, are related to the disordered B2 structure.

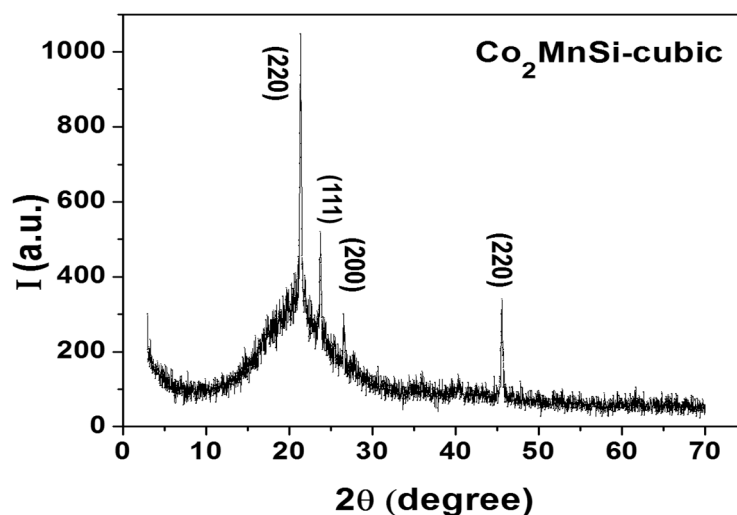


Figure 2. X-ray diffraction pattern of Co_2MnSi glass-coated microwire measured at room temperature.

By using the formula reported in [33], we estimated the nanocrystalline grain size, D_g , related to each peak as listed in Table 1.

Table 1. Average grain size (nm) of as-cast Co_2MnSi glass-coated microwire.

Peak Position 2θ ($^\circ$)	FWHM B_{size} ($^\circ$)	D_g (nm)
45.6	0.17	53.9
21.4	0.21	40.3
23.7	0.20	44.0

3.2. Magnetic Properties

3.2.1. Room Temperature Magnetic Properties

The hysteresis (M-H) loops of as-prepared Co_2MnSi glass-coated microwire measured at room temperature for two different applied external magnetic field directions to check the magnetic anisotropy are shown in Figure 3. First, the direction where the external magnetic field is applied is parallel to the axis of the Co_2MnSi glass-coated microwire, i.e., $\theta = 0^\circ$ (in plane) and the other direction is perpendicular to the axis of the Co_2MnSi glass-coated microwire, i.e., $\theta = 90^\circ$ (out of plane). As expected, the sample exhibited ferromagnetic behavior as the transition to the paramagnetic phase for the Co_2MnSi alloy is above room temperature ($T_c = 985 \text{ K}$) [11]. For easy comparison, all hysteresis loops are normalized to the maximum magnetic moment. As observed in Figure 3, the Co_2MnSi glass-coated microwire shows strong axial magnetic anisotropy where the axial hysteresis loop shows a squared shape with high magnetic remanence magnetization, whereas the out-of-axis hysteresis loop shows a linear shape with a remanence magnetization near to zero (see the inset of Figure 3). Thus, the easy magnetization direction is parallel to the microwire axis, and the hard magnetization direction is in the perpendicular direction. The behavior of both the axial and the out-of-axis hysteresis loops indicates the existence of magnetic anisotropy.

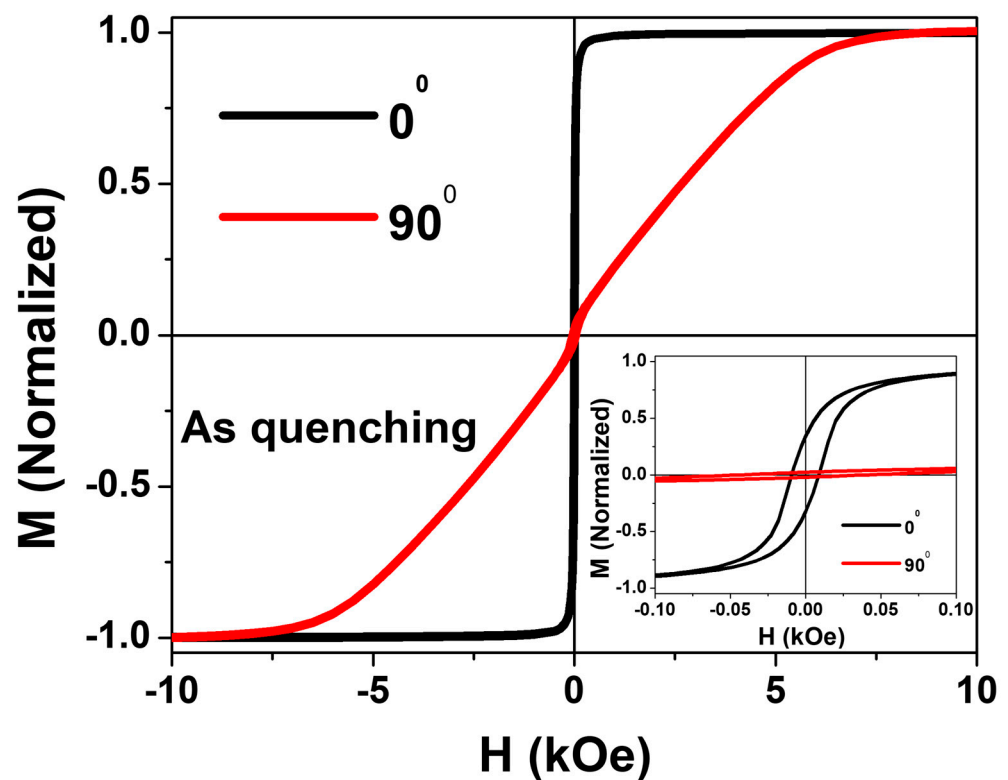


Figure 3. The in-plane (parallel to wire axis, black loop) and out-of-plane (perpendicular to the wire axis, red loop) hysteresis loops of as-prepared Co_2MnSi glass-coated microwires measured at room temperature. The inset indicates the loops with low scale of the applied magnetic field.

There are two main sources of this strong magnetic anisotropy, the cubic magnetocrystalline anisotropy and the uniaxial magnetic anisotropy due to the existence of crystalline phases and the shape of the magnetic anisotropy of the microwire, respectively [43,44]. As shown in the inset of Figure 3, the axial hysteresis loop does not show a perfectly squared shape as reported for the anisotropic materials. In our case, the non-perfect squared hysteresis loop can be attributed to the existence of the amorphous and crystalline phases. Noteworthy, same observation has recently been observed in our previous work on Co_2 -

based Heusler alloy glass-coated microwires [27]. In addition, these observations agree with results obtained elsewhere for Co₂MnSi-based Heusler alloy thin films [43].

3.2.2. Temperature Dependence of Magnetic Behavior

Magnetic behavior of the as-prepared Co₂MnSi glass-coated microwires at different temperatures is provided in Figures 4 and 5.

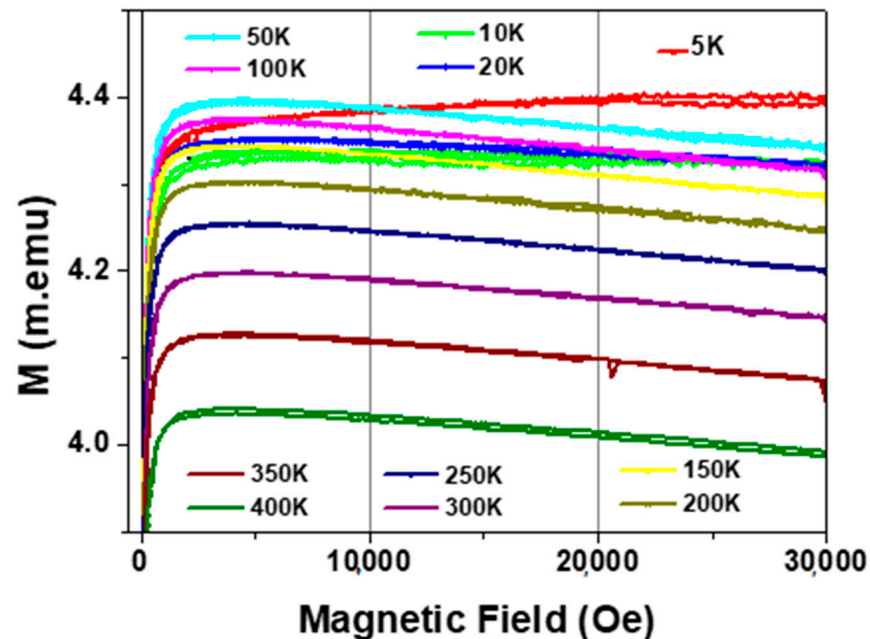


Figure 4. Magnetization vs. magnetic field curves of as-prepared Co₂MnSi glass-coated microwires. All loops have been measured at a temperature range from 400 K to 5 K.

In Figure 4, we focus on the part of the hysteresis loops that illustrates the increase of the saturation field for all samples with temperature. The saturation magnetic field, H_{sat} , shows unusual behavior with temperature and magnetic field. A monotonic increase in the saturation magnetic field by decreasing the temperature from 400 K to 50 K is observed. Then, H_{sat} begins to decrease upon decreasing the temperature from 50 K to 10 K. Finally, an additional H_{sat} increase by decreasing the temperature from 10 K to 5 K is observed. The maximum saturation magnetic field is observed at $T = 50$ K for the magnetic field (H) range $0 \leq H \leq 10,000$ Oe. The variation of saturation field with temperature can be attributed to the change in the magnetic microstructure of Co₂MnSi by decreasing the temperature. In addition, the changing of the internal stresses originated by the glass cover layer with temperature leads to modification of the microstructure of the sample, which directly affects the magnetic response. Furthermore, the antiferromagnetic coupling of Mn-Mn, which appears for the temperatures below the room temperature, adds an additional effect in changing the magnetic behavior of the Co₂MnSi with temperature. On the other hand, the diamagnetic contribution of the glass-coating can affect the hysteresis loops character providing a negative slope on M-H loops above the saturation.

The saturation magnetic field for temperature ranges below 50 K shows non-uniform magnetic behavior compared with the measuring loops at T values higher than 50 K. The saturation field curves show a notable negative slope for the magnetic curves measured at 20, 10 and 5 K. As depicted in Figure 4, the maximum saturation field is observed at 5 K for the magnetic field (H) range $10 < H \leq 50$ (kOe). This observation can be related to the strong antiferromagnetic behavior of Mn-Mn at low temperatures.

Figure 5 illustrates the hysteresis loops of Co₂MnSi glass-coated microwires measured in the temperature range from 400 to 50 K. All measured hysteresis loops do not show a notable magnetic change, where the average values of the coercivity and normalized

magnetic remanence do not show a strong change with temperature (see Figure 6). The difference between the highest value and the lowest value of the coercivity and the normalized remanence is 5 Oe and 0.08, respectively. This observation is different from the one that we reported for Co_2FeSi glass-coated microwires, in which we observed a strong dependence of the coercivity and remanence on temperature, as reported in Ref. [27]. We illustrated that the competition between different kinds of magnetic anisotropy, i.e., the uniaxial magnetic anisotropy, cubic magnetocrystalline anisotropy and their temperature dependence led to the anomalous magnetic behavior of the coercivity and remanence with temperature. In the current case, we suppose a weak dependence for both types of the magnetic anisotropy on the temperature. Thus, roughly a stable magnetic behavior with temperature is observed.

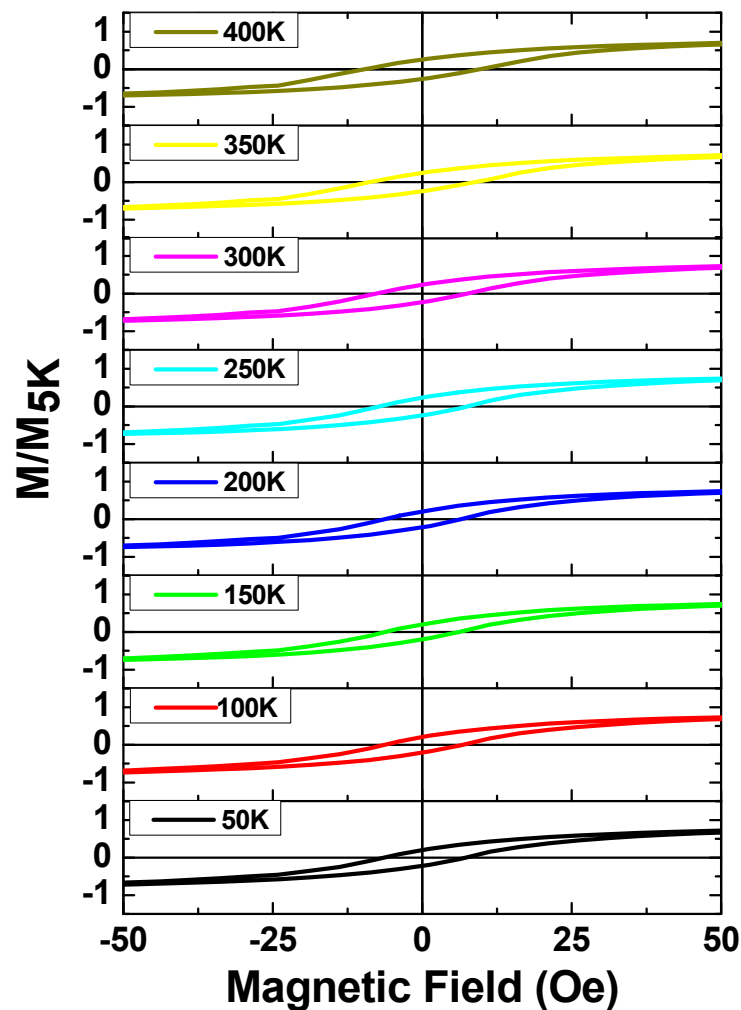


Figure 5. Hysteresis loops, measured in an applied magnetic field parallel to the axis of the microwires at different temperatures from 50 K to 400 K for as-prepared Co_2MnSi glass-coated microwires.

It is important to evaluate the complete magnetic behavior with temperature in order to check its thermal stability, which it is an important physical property to determine its potential for spintronics application. In addition, the temperature dependence can provide useful information on the possibility for the magnetic phase transition. Thus, we measured the magnetization dependence on temperature (M vs. T), i.e., zero field cooling, (ZFC) and field cooling (FC), at low magnetic field ($H = 100$ Oe) and temperature range from 5 to 350 K, as plotted in Figure 7. In the field cooling protocol, the as-prepared Co_2MnSi glass-coated microwires were cooled down to 5 K under an applied magnetic field ($H = 100$ Oe), which caused the random magnetic moment vectors to freeze parallel to the applied field

at low temperatures. However, the M-H loops show a thermal magnetic stability (M vs. T) for both ZFC and FC magnetization curves that show strong irreversibility magnetic behavior with a blocking temperature at 150 K. Such magnetic irreversibility has been detected in Co₂-based Heusler alloy glass-coated microwires [27]. This irreversibility strongly depends on the micromagnetic structure of the magnetic materials. In addition, it appears to be owing to the coexistence of typical re-entrant ferromagnetism and spin glass-type behavior, as reported elsewhere [45]. Moreover, the disordered structure (B2 phase) and chemical composition of the Co₂MnSi glass-coated microwires affects the irreversibility behavior where the magnetic ground state is not purely ferromagnetic but has a strong antiferromagnetic contribution, especially at low temperature for Mn-Mn interaction; random spin disorder (B2 phase) is also found with the ferromagnetic order (L2₁ phase) [11,46].

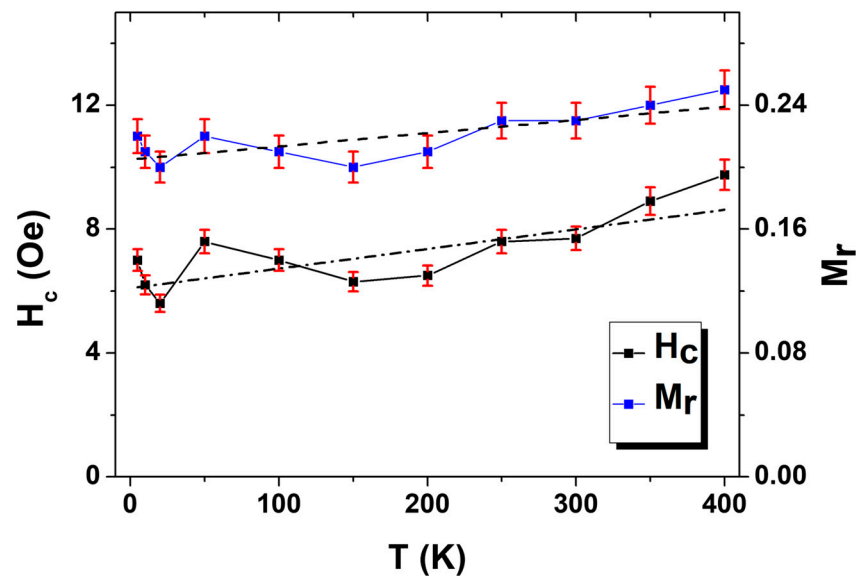


Figure 6. Temperature dependencies of coercivity (H_c) and normalized remanence (M_r) of as-prepared Co₂MnSi glass-coated microwires. (Dashed lines indicates the liner fitting).

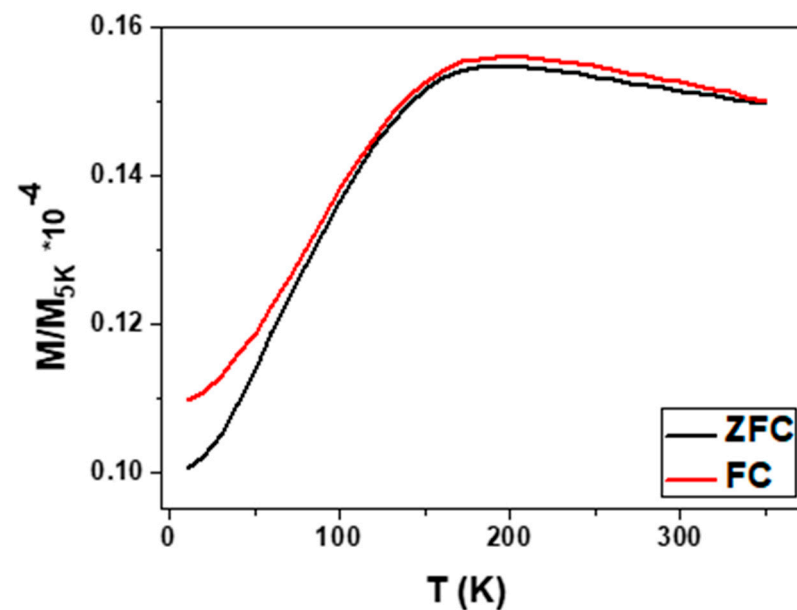


Figure 7. Zero field cooling (ZFC) and field cooling (FC) of as-prepared Co₂MnSi glass-coated microwires.

4. Discussion

The main features of the magneto-structural properties of Co₂MnSi glass-coated microwires comes from the fabrication process where Co₂MnSi Heusler compounds prepared with different form and technique (thin films, bulk and ribbons) does not show similar magneto-structural behavior at the same conditions [11–16]. As we described above, the main peculiarity of the Taylor–Ulitsky method for preparing Heusler-alloy-based glass-coated microwires is the simultaneous rapid solidification of the metallic nucleus surrounded by the glass coating [24,27,47]. Therefore, strong mechanical internal stresses are induced and distributed in a complex and inhomogeneous way within the metallic nucleus radius of the glass-coated microwires. Thus, near to the axis of the metallic nucleus the tensile stresses are the strongest. Meanwhile closer to the interface layer with the glass coating the compressive stresses are dominant [38,48,49].

Mainly, there are three main sources of internal stresses, σ_i , in glass-coated microwires: (1) The quenching internal stresses, which are related to the rapid solidification of the metallic nucleus alloy. (2) The stresses originating from the difference in thermal expansion coefficients of the metallic nucleus alloy and glass. (3) Finally, the drawing stresses originating from the drawing of the composite microwire are present [48,49]. In glass-coated microwires the solidification of the metallic nucleus alloys in the presence of glass-coating is the main source of the quenching internal stress from the wire surface towards the microwire axis. By considering successive concentric cylindrical shells solidifying consecutively starting from the outside, due to the temperature gradient at the glass transition temperature, one can easily evaluate such internal stress components, as reported elsewhere [49,50]. The largest internal stresses were those related to the difference in thermal expansion coefficients of the metallic alloy and the glass: the σ_i value up to 4 GPa [26,38,41,49,50]. Additionally, the axial σ_i component, σ_z , is affected by the ρ -ratio given as d/D , as follows from the most simplified approximation, σ_i given as [26,41,49]:

$$\sigma_z = P(k + 1)\Delta + 2/(k\Delta + 1) \quad (1)$$

$$\sigma_\varphi = \sigma_r = P = \varepsilon E k \Delta / (k/3 + 1)\Delta + 4/3 \quad (2)$$

where σ_r and σ_φ are radial and circular stresses, respectively. $\Delta = (1 - \rho^2)/\rho^2$, $k = E_{\text{glass}}/E_{\text{metallic}}$, E_{metallic} , E_{glass} —Young modulus of metallic nucleus alloy and glass cover layer, respectively, $\varepsilon = (\alpha_m - \alpha_g)(T_m - T_{\text{room}})$, α_{metallic} , α_{glass} are thermal expansion coefficients of metallic nucleus alloy and glass cover layer, respectively, and T_m , T_{room} are melting and room temperatures.

Consequently, the uniaxial magnetic anisotropy in Co₂MnSi glass-coated microwires must be associated with the internal stresses together with the magnetostriction coefficient, λ_s , of Co₂-based alloys [26,27,31–33,41]. Therefore, rather strong internal stresses associated with the presence of glass coatings during the fabrication process can be the origin of the appearance of a disordered structure phase (B2) besides the ordered one (L2₁) and amorphous one (as explained in the XRD analysis see Figure 2 and Table 1). Such a structure is responsible for the in-plane uniaxial magnetic anisotropy at room temperature beside the large irreversible magnetic behavior below the room temperature.

Additionally, strong internal stresses can hinder the crystallization process [26,42] and the nanocrystalline structure of the as-prepared and even annealed Co₂MnSi glass-coated microwires can be related to the presence of such stresses.

On the other hand, Heusler alloys are usually brittle and therefore present poor mechanical properties [20]. Generally, poor mechanical properties became a problem for use of conventional methods for the preparation of low dimensional Heusler alloys [20]. In this sense, the use of the Taylor–Ulitsky method provides several advantages:

- (i) Presence of flexible glass coating can improve the mechanical properties of glass-coated microwires [42]
- (ii) Proposed method allows preparation of thin Heusler alloy microwires by single step preparation method, directly in the form of a microwire.

5. Conclusions

In conclusion, we highlighted the fabrication and magneto-structural characterization of well-known Co₂ Heusler alloy (Co₂MnSi)-based glass-coated microwires. The magnetic characterization has been performed for a wide range of temperature 5 to 400 K. Soft magnetic behavior has been reported with maximum H_c = 9 Oe at (T = 400 K). At room temperature, the as-prepared sample shows strong in-plane uniaxial magnetic anisotropy parallel to the microwire axis. The M-H loops show a stable magnetic behavior with changing the temperature, where no notable change has been observed. Large irreversibility has been detected below the room temperature with blocking temperature at T = 150 K. The structure investigation proves a well-defined crystalline structure with a lattice parameter $a = 5.62 \text{ \AA}$. In addition, the existence of the disordered B2 and amorphous structures has been observed. The grain size evaluation proves the existence of nanocrystalline grain size ($D_g = 46 \text{ nm}$). Moreover, we have illustrated that the strong internal stresses, which are induced by the solidification process during the fabrication process, play a main role in the magnetic structural properties. Future research is necessary to explain the effects of annealing conditions and geometrical parameters on the magneto-structural and thermoelectric properties. From the application viewpoint, our findings are important, which paves the way for a large-scale production of high-performance Co₂-based nanocrystalline soft magnetic Heusler-alloy-based glass-coated microwires for a variety of industrial applications.

Author Contributions: Conceptualization, M.S. and A.Z.; methodology, V.Z. and A.T.; validation, M.S., V.Z. and A.Z.; formal analysis, M.S. and A.T.; investigation, M.S., A.Z., V.Z. and A.T.; resources, V.Z. and A.Z.; data curation, M.I. and A.T.; writing—original draft preparation, M.S. and A.Z.; writing—review and editing, M.S. and A.Z.; visualization, M.S., M.I. and A.T.; supervision, A.Z.; project administration, V.Z. and A.Z.; funding acquisition, V.Z. and A.Z. All authors have read and agreed to the published version of the manuscript.

Funding: This research was funded by the Spanish MCIU, under PGC2018-099530-B-C31 (MCIU/AEI/FEDER, UE), by EU under “INFINITE” (Horizon 2020) project, by the Government of the Basque Country, under PUE_2021_1_0009 and Elkartek (MINERVA and ZE-KONP) projects and by under the scheme of “Ayuda a Grupos Consolidados” (Ref.: IT1670-22), by the University of Basque Country under the COLAB20/15 project and by the Diputación Foral de Gipuzkoa in the frame of Programa “Red Guipuzcoana de Ciencia, Tecnología e Innovación 2021” under 2021-CIEN-000007-01 project. We also wish to thank the administration of the University of the Basque Country, which not only provides very limited funding, but even expropriates the resources received by the research group from private companies for the research activities of the group. Such interference helps keep us on our toes.

Data Availability Statement: Not applicable.

Acknowledgments: The authors are thankful for the technical and human support provided by SGiker of UPV/EHU (Medidas Magnéticas Gipuzkoa) and European funding (ERDF and ESF).

Conflicts of Interest: The authors declare no conflict of interest.

References

1. Inomata, K.; Ikeda, N.; Tezuka, N.; Goto, R.; Sugimoto, S.; Wojcik, M.; Jedryka, E. Highly Spin-Polarized Materials and Devices for Spintronics. *Adv. Mater.* **2008**, *9*, 14101. [[CrossRef](#)] [[PubMed](#)]
2. Chumak, O.M.; Pacewicz, A.; Lynnyk, A.; Salski, B.; Yamamoto, T.; Seki, T.; Domagala, J.Z.; Głowiński, H.; Takanashi, K.; Baczewski, L.T.; et al. Magnetoelastic Interactions and Magnetic Damping in Co₂Fe_{0.4}Mn_{0.6}Si and Co₂FeGa_{0.5}Ge_{0.5} Heusler Alloys Thin Films for Spintronic Applications. *Sci. Rep.* **2021**, *11*, 7608. [[CrossRef](#)] [[PubMed](#)]
3. De Groot, R.A.; Mueller, F.M.; Engen, P.G.V.; Buschow, K.H.J. New Class of Materials: Half-Metallic Ferromagnets. *Phys. Rev. Lett.* **1983**, *50*, 2024. [[CrossRef](#)]
4. Elphick, K.; Frost, W.; Samiepour, M.; Kubota, T.; Takanashi, K.; Sukegawa, H.; Mitani, S.; Hirohata, A. Heusler Alloys for Spintronic Devices: Review on Recent Development and Future Perspectives. *Sci. Technol. Adv. Mater.* **2021**, *22*, 235–271. [[CrossRef](#)]
5. Bai, Z.; Shen, L.E.I.; Han, G.; Feng, Y.P. Data Storage: Review of Heusler Compounds. *Spin* **2012**, *2*, 1230006. [[CrossRef](#)]
6. Galanakis, I.; Dederichs, P.H.; Papanikolaou, N. Slater-Pauling Behavior and Origin of the Half-Metallicity of the Full-Heusler Alloys. *Phys. Rev. B* **2002**, *66*, 174429. [[CrossRef](#)]

7. Hazra, B.K.; Kaul, S.N.; Srinath, S.; Raja, M.M. Uniaxial Anisotropy, Intrinsic and Extrinsic Damping in Co₂FeSi Heusler Alloy Thin Films. *J. Phys. D Appl. Phys.* **2019**, *52*, 325002. [[CrossRef](#)]
8. Wurmehl, S.; Fecher, G.H.; Kandpal, H.C.; Ksenofontov, V.; Felser, C.; Lin, H.J.; Morais, J. Geometric, Electronic, and Magnetic Structure of Co₂FeSi: Curie Temperature and Magnetic Moment Measurements and Calculations. *Phys. Rev. B Condens. Matter. Mater. Phys.* **2005**, *72*, 184434. [[CrossRef](#)]
9. Li, P.; Koo, J.; Ning, W.; Li, J.; Miao, L.; Min, L.; Zhu, Y.; Wang, Y.; Alem, N.; Liu, C.X.; et al. Giant Room Temperature Anomalous Hall Effect and Tunable Topology in a Ferromagnetic Topological Semimetal Co₂MnAl. *Nat. Commun.* **2020**, *11*, 3476. [[CrossRef](#)]
10. Belopolski, I.; Manna, K.; Sanchez, D.S.; Chang, G.; Ernst, B.; Yin, J.; Zhang, S.S.; Cochran, T.; Shumiya, N.; Zheng, H.; et al. Discovery of Topological Weyl Fermion Lines and Drumhead Surface States in a Room Temperature Magnet. *Science* **2019**, *365*, 1278–1281. [[CrossRef](#)]
11. Ahmed, S.J.; Boyer, C.; Niewczas, M. Magnetic and Structural Properties of Co₂MnSi Based Heusler Compound. *J. Alloy. Compd.* **2019**, *781*, 216–225. [[CrossRef](#)]
12. Guillemard, C.; Petit-Watelot, S.; Pasquier, L.; Pierre, D.; Ghanbaja, J.; Rojas-Sánchez, J.C.; Bataille, A.; Rault, J.; le Fèvre, P.; Bertran, F.; et al. Ultralow Magnetic Damping in Co₂Mn-Based Heusler Compounds: Promising Materials for Spintronics. *Phys. Rev. Appl.* **2019**, *11*, 064009. [[CrossRef](#)]
13. Liu, H.X.; Honda, Y.; Taira, T.; Matsuda, K.I.; Arita, M.; Uemura, T.; Yamamoto, M. Giant Tunneling Magnetoresistance in Epitaxial Co₂MnSi/MgO/Co₂MnSi Magnetic Tunnel Junctions by Half-Metallicity of Co₂MnSi and Coherent Tunneling. *Appl. Phys. Lett.* **2012**, *101*, 132418. [[CrossRef](#)]
14. Stuelke, L.; Kharel, P.; Shand, P.M.; Lukashev, P.V. First Principles Study of Perpendicular Magnetic Anisotropy in Thin-Film Co₂MnSi. *Phys. Scr.* **2021**, *96*, 125818. [[CrossRef](#)]
15. Ishida, S.; Fujii, S.; Kashiwagi, S.; Asano, S. Search for Half-Metallic Compounds in Co₂MnZ (Z = IIIb, IVb, Vb Element). *J. Phys. Soc. Jpn.* **1995**, *64*, 2152–2157. [[CrossRef](#)]
16. Pradines, B.; Arras, R.; Abdallah, I.; Biziere, N.; Calmels, L. First-Principles Calculation of the Effects of Partial Alloy Disorder on the Static and Dynamic Magnetic Properties of Co₂MnSi. *Phys. Rev. B* **2017**, *95*, 094425. [[CrossRef](#)]
17. Cheng, S.F.; Nadgorny, B.; Bussmann, K.; Carpenter, E.E.; Das, B.N.; Trotter, G.; Raphael, M.P.; Harris, V.G. Growth and Magnetic Properties of Single Crystal Co₂MnX (X = Si, Ge) Heusler Alloys. *IEEE Trans. Magn.* **2001**, *37*, 2176–2178. [[CrossRef](#)]
18. Jourdan, M.; Minár, J.; Braun, J.; Kronenberg, A.; Chadov, S.; Balke, B.; Gloskovskii, A.; Kolbe, M.; Elmers, H.J.; Schönhense, G.; et al. Direct Observation of Half-Metallicity in the Heusler Compound Co₂MnSi. *Nat. Commun.* **2014**, *5*, 3974. [[CrossRef](#)]
19. Wang, B.; Liu, Y. Exchange Bias and Inverse Magnetocaloric Effect in Co and Mn Co-Doped Ni₂MnGa Shape Memory Alloy. *Metals* **2013**, *3*, 69–76. [[CrossRef](#)]
20. Dunand, D.C.; Müllner, P. Size Effects on Magnetic Actuation in Ni-Mn-Ga Shape-Memory Alloys. *Adv. Mater.* **2011**, *23*, 216–232. [[CrossRef](#)]
21. Felser, C.; Hirohata, A. (Eds.) *Heusler Alloys Properties, Growth, Applications*; Springer Series in Materials Science; Springer International Publishing: Cham, Switzerland, 2016; Volume 222, ISBN 978-3-319-21448-1.
22. Alam, J.; Bran, C.; Chiriac, H.; Lupu, N.; Övári, T.A.; Panina, L.V.; Rodionova, V.; Varga, R.; Vazquez, M.; Zhukov, A. Cylindrical Micro and Nanowires: Fabrication, Properties and Applications. *J. Magn. Magn. Mater.* **2020**, *513*, 167074. [[CrossRef](#)]
23. Salaheldeen, M.; Abu-Dief, A.M.; Martínez-Goyeneche, L.; Alzahrani, S.O.; Alkhatib, F.; Álvarez-Alonso, P.; Blanco, J.Á. Dependence of the Magnetization Process on the Thickness of Fe70Pd30 Nanostructured Thin Film. *Materials* **2020**, *13*, 5788. [[CrossRef](#)] [[PubMed](#)]
24. Zhukov, A.; Rodionova, V.; Ilyn, M.; Aliev, A.M.; Varga, R.; Michalik, S.; Aronin, A.; Abrosimova, G.; Kiselev, A.; Ipatov, M.; et al. Magnetic Properties and Magnetocaloric Effect in Heusler-Type Glass-Coated NiMnGa Microwires. *J. Alloy. Compd.* **2013**, *575*, 73–79. [[CrossRef](#)]
25. Mallick, S.; Mondal, S.; Seki, T.; Sahoo, S.; Forrest, T.; Maccherozzi, F.; Wen, Z.; Barman, S.; Barman, A.; Takanashi, K.; et al. Tunability of Domain Structure and Magnonic Spectra in Antidot Arrays of Heusler Alloy. *Phys. Rev. Appl.* **2019**, *12*, 014043. [[CrossRef](#)]
26. Zhukov, A.; Corte-Leon, P.; Gonzalez-Legarreta, L.; Ipatov, M.; Blanco, J.M.; Gonzalez, A.; Zhukova, V. Advanced Functional Magnetic Microwires for Technological Applications. *J. Phys. D Appl. Phys.* **2022**, *55*, 253003. [[CrossRef](#)]
27. Salaheldeen, M.; Garcia-Gomez, A.; Ipatov, M.; Corte-Leon, P.; Zhukova, V.; Blanco, J.M.; Zhukov, A. Fabrication and Magneto-Structural Properties of Co₂-Based Heusler Alloy Glass-Coated Microwires with High Curie Temperature. *Chemosensors* **2022**, *10*, 225. [[CrossRef](#)]
28. Zhukov, A.; Garcia, C.; Ilyn, M.; Varga, R.; del Val, J.J.; Granovsky, A.; Rodionova, V.; Ipatov, M.; Zhukova, V. Magnetic and transport properties of granular and Heusler-type glass-coated microwires. *J. Magn. Magn. Mater.* **2012**, *324*, 3558–3562. [[CrossRef](#)]
29. Shevyrtalov, S.; Rodionova, V.; Lyatun, I.; Zhukova, V.; Zhukov, A. Post-Annealing Influence on Magnetic Properties of Rapidly Quenched Ni-Mn-Ga Glass-Coated Microwires. *IEEE Trans. Magn.* **2021**, *57*, 2000706. [[CrossRef](#)]
30. Garcia, C.; Zhukova, V.; Shevyrtalov, S.; Ipatov, M.; Corte-Leon, P.; Zhukov, A. Tuning of Magnetic Properties in Ni-Mn-Ga Heusler-Type Glass-Coated Microwires by Annealing. *J. Alloy. Compd.* **2020**, *838*, 155481. [[CrossRef](#)]

31. Salaheldeen, M.; Garcia-Gomez, A.; Corte-Leon, P.; Ipatov, M.; Zhukova, V.; Gonzalez, J.; Zhukov, A. Anomalous Magnetic Behavior in Half-Metallic Heusler Co_2FeSi Alloy Glass-Coated Microwires with High Curie Temperature. *J. Alloy. Compd.* **2022**, *923*, 166379. [[CrossRef](#)]
32. Salaheldeen, M.; Garcia-Gomez, A.; Corte-León, P.; Gonzalez, A.; Ipatov, M.; Zhukova, V.; Gonzalez, J.M.; López Antón, R.; Zhukov, A. Manipulation of Magnetic and Structure Properties of Ni_2FeSi Glass-Coated Microwires by Annealing. *SSRN Electron. J.* **2022**. [[CrossRef](#)]
33. Salaheldeen, M.; Garcia, A.; Corte-Leon, P.; Ipatov, M.; Zhukova, V.; Zhukov, A. Unveiling the Effect of Annealing on Magnetic Properties of Nanocrystalline Half-Metallic Heusler Co_2FeSi Alloy Glass-Coated Microwires. *J. Mater. Res. Technol.* **2022**, *20*, 4161–4172. [[CrossRef](#)]
34. Mitxelena-Iribarren, O.; Campisi, J.; de Apellániz, I.M.; Lizarbe-Sancha, S.; Arana, S.; Zhukova, V.; Mujika, M.; Zhukov, A. Glass-Coated Ferromagnetic Microwire-Induced Magnetic Hyperthermia for in Vitro Cancer Cell Treatment. *Mater. Sci. Eng. C* **2020**, *106*, 110261. [[CrossRef](#)] [[PubMed](#)]
35. Talaat, A.; Alonso, J.; Zhukova, V.; Garaio, E.; García, J.A.; Srikanth, H.; Phan, M.H.; Zhukov, A. Ferromagnetic Glass-Coated Microwires with Good Heating Properties for Magnetic Hyperthermia. *Sci. Rep.* **2016**, *6*, 39300. [[CrossRef](#)]
36. Kozejova, D.; Fecova, L.; Klein, P.; Sabol, R.; Hudak, R.; Sulla, I.; Mudronova, D.; Galik, J.; Varga, R. Biomedical Applications of Glass-Coated Microwires. *J. Magn. Magn. Mater.* **2019**, *470*, 2–5. [[CrossRef](#)]
37. Zhukov, A.; Ipatov, M.; Corte-Leon, P.; Blanco, J.M.; Zhukova, V. Advanced Functional Magnetic Microwires for Magnetic Sensors Suitable for Biomedical Applications. In *Magnetic Materials and Technologies for Medical Applications*; Tishin, A.M., Ed.; Elsevier: Amsterdam, The Netherlands, 2022; pp. 527–579. [[CrossRef](#)]
38. Aronin, A.S.; Abrosimova, G.E.; Kiselev, A.P.; Zhukova, V.; Varga, R.; Zhukov, A. The effect of mechanical stress on $\text{Ni}_{63.8}\text{Mn}_{11.1}\text{Ga}_{25.1}$ microwire crystalline structure and properties. *Intermetallics* **2013**, *43*, 60–64. [[CrossRef](#)]
39. Zhukova, V.; Cobeño, A.F.; Zhukov, A.; de Arellano Lopez, A.R.; López-Pombero, S.; Blanco, J.M.; Larin, V.; Gonzalez, J. Correlation between magnetic and mechanical properties of devitrified glass-coated $\text{Fe}_{71.8}\text{Cu}_1\text{Nb}_{3.1}\text{Si}_{15}\text{B}_{9.1}$ microwires. *J. Magn. Magn. Mater.* **2002**, *249*, 79–84. [[CrossRef](#)]
40. Zhukov, A.; Ipatov, M.; del Val, J.J.; Zhukova, V.; Chernenko, V.A. Magnetic and Structural Properties of Glass-Coated Heusler-Type Microwires Exhibiting Martensitic Transformation. *Sci. Rep.* **2018**, *8*, 621. [[CrossRef](#)]
41. Zhukova, V.; Corte-Leon, P.; Blanco, J.M.; Ipatov, M.; Gonzalez-Legarreta, L.; Gonzalez, A.; Zhukov, A. Development of Magnetically Soft Amorphous Microwires for Technological Applications. *Chemosensors* **2022**, *10*, 26. [[CrossRef](#)]
42. Zhukov, A.; Ipatov, M.; Talaat, A.; Blanco, J.M.; Hernando, B.; Gonzalez-Legarreta, L.; Suñol, J.J.; Zhukova, V. Correlation of Crystalline Structure with Magnetic and Transport Properties of Glass-Coated Microwires. *Crystals* **2017**, *7*, 41. [[CrossRef](#)]
43. Guo, X.B.; Zuo, Y.L.; Cui, B.S.; Li, D.; Yun, J.J.; Wu, K.; Wang, T.; Xi, L. Post Annealing Induced Magnetic Anisotropy in CoFeSi Thin Films on MgO (001). *J. Phys. D Appl. Phys.* **2017**, *50*, 085006. [[CrossRef](#)]
44. Velázquez, J.; Vázquez, M.; Hernando, A.; Savage, H.T.; Wun-Fogle, M. Magnetoelastic anisotropy in amorphous wires due to quenching. *J. Appl. Phys.* **1991**, *70*, 6525–6527. [[CrossRef](#)]
45. Gunnarsson, K.; Svedlindh, P.; Andersson, J.O.; Nordblad, P.; Lundgren, L.; Aruga Katori, H.; Ito, A. Magnetic Behavior of a Reentrant Ising Spin Glass. *Phys. Rev. B* **1992**, *46*, 8227–8231. [[CrossRef](#)] [[PubMed](#)]
46. Yang, F.; Li, W.; Li, J.; Chen, H.; Liu, D.; Chen, X.; Yang, C. The Microstructure and Magnetic Properties of Co_2MnSi Thin Films Deposited on Si Substrate. *J. Alloy. Compd.* **2017**, *723*, 188–191. [[CrossRef](#)]
47. Zhukova, V.; Chernenko, V.; Ipatov, M.; Zhukov, A. Magnetic Properties of Heusler-Type NiMnGa Glass-Coated Microwires. *IEEE Trans. Magn.* **2015**, *51*, 501604. [[CrossRef](#)]
48. Chiriac, H.; Vári, T.A.; Pop, G. Internal Stress Distribution in Glass-Covered Amorphous Magnetic Wires. *Phys. Rev. B* **1995**, *52*, 10104. [[CrossRef](#)]
49. Torcunov, A.V.; Baranov, S.A.; Larin, V.S. The Internal Stresses Dependence of the Magnetic Properties of Cast Amorphous Microwires Covered with Glass Insulation. *J. Magn. Magn. Mater.* **1999**, *196–197*, 835–836. [[CrossRef](#)]
50. Chiriac, H.; Lupu, N.; Stoian, G.; Ababei, G.; Corodeanu, S.; Óvári, T.A. Ultrathin Nanocrystalline Magnetic Wires. *Crystals* **2017**, *7*, 48. [[CrossRef](#)]